An Investigation on Spot Weld Modelling for Crash Simulation with LS-DYNA

F. Seeger [a], M. Feucht [a], Th. Frank [a], B. Keding [b], A. Haufe [b]

[a] DaimlerChrysler AG, EP/SPB, HPC X411, 71059 Sindelfingen, Germany
{falko.seeger, markus.feucht, thomas.frank}@daimlerchrysler.com

[b] DYNAmore GmbH, Industriestr. 2, 70565 Stuttgart, Germany
{bastian.keding, andre.haufe}@dynamore.de

Abstract:

Because of weight reduction necessities, high-strength steels are more and more widely used in body-in-white (BiW) structures in recent years. Concerning the behaviour of such structures during a car crash the joints between high-strength materials are seen as critical points. Therefore the properties of welded joints, especially the failure behaviour at high velocities have to be taken into consideration during the development phase.

In this paper, we present an overview on the current activities at the DaimlerChrysler AG regarding investigations on spot weld failure behaviour. A suitable model that is able to represent the failure behaviour of spot welds in BiW structures and that is independent of mesh sensitivity has been developed. An elasto-plastic material model based on von Mises plasticity (MAT_100) has been further enhanced with a new failure criterion. The model has been implemented into LS-DYNA. The material as well as the failure behaviour is verified and calibrated through precision experiments conducted on specimen level and later validated on component level.

Keywords:

Spot weld modeling, constitutive model and failure, crashworthiness, connection modelling, finite elements

1   Introduction

Since years various efforts have been made to identify suitable strategies to model spot weld or connections in general in commercial FE-codes (see [1]-[5]). The rather simplistic modelling techniques in crashworthiness using tied-contacts or rigid connections were improved by applying deformable spot weld elements which take into account the stiffness of the connection itself. The latter modelling technique uses a combination of tied contacts and structural elements such as beams or one or more solid elements. This approach worked sufficiently well even though obvious simplifications such as the negligence of anisotropy in the elements were made. One of the main reasons for this satisfactory performance was the assumption that the spot weld itself does not fail in case of crash impacts but rather the material which is connected by the spot weld. This assumption was based on experimental testing and holds true for ductile steels. However, this picture changes substantially with the use of high-strength steels. Now, rather the spot weld itself is failing than the material surrounding the spot weld. As a consequence, the models using solely deformable structural elements needed improvement in order to predict the correct failure behaviour of the connections in complex car crash scenarios.

The present paper will investigate different modelling techniques used for connections in LS-DYNA [6]. The merits and limits of the widely used methods will be evaluated by using data from simple experimental tests. A suitable model that is able to represent the failure behaviour of spot welds in BiW structures and which is independent of mesh sensitivity, has been developed. An elasto-plastic material model based on MAT_100 has been further enhanced with a new failure criterion. The model has been implemented into LS-DYNA. The material as well as the failure behaviour is verified and calibrated through precision experiments conducted on specimen level and later validated on component level.

In addition, very recent developments in LS-DYNA will be discussed which enhance the modelling capabilities in LS-DYNA for connections between high strength steel sheets dramatically. This improved performance will be illustrated using experimental data from component testing.

2   Experimental basis

2.1   Motivation

As mentioned above, the goal of our investigation is to develop a suitable model to cover the failure behaviour of spot weld connections in car crash simulations. As the result of continually rising computational power the model size represented by the number of finite elements increased and at the same time the element size in car models was getting smaller in recent years. Today a car model consist of up to 1 200 000 finite elements with 5-15mm per element edge. Considering the over-all car simulation the FE-model is relatively fine, but in comparison to the dimension of individual spot welds the discretization is rather coarse. Typically the spot weld is to be modelled by one element, e.q. a hexahedron or beam element, due to time step constraints. However, if only one element is available to cover the material as well as the failure behaviour, specially adapted experiments which provide the basis for investigation, verification, calibration and validation of new spot weld models are needed. Such experiments should combine the realistic behaviour of the spot weld as observed in a real car and the simplicity to model various failure mechanisms separately.

2.2   Specimen Level

On specimen level three different experimental setups were considered: First KSII-specimen, which have been developed by [1], secondly simple lap shear specimen and finally a peel test specimen, see Fig. 1, Fig. 2 and Fig. 3, respecively. The single parts are attached by only one spot weld.

The KSII-experiments, conducted with loading angles of 0°, 30°, 60° and 90°, are essential to derive the relationship between normal and shear stress. With 90° only normal stresses occur in the spot weld, whereas mainly shear stress is expected for the 0° load case. These experiments are used to calibrate the material and failure parameters.

Furthermore, the peel test specimen is useful for checking the spot weld behaviour under bending respectively peeling conditions. This experiment is also used for calibration.

A first validation of the numerical model can be performed on basis of the lap shear specimen. Due to the load case a multi-axial stress state as a combination of shear, normal and bending stresses arises. It is therefore a simple yet useful setup to validate calibrated models and evaluate the chosen strategy.
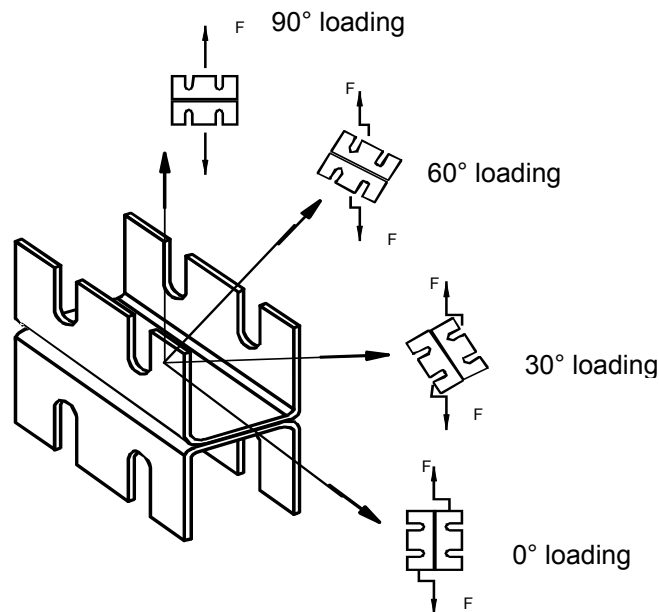
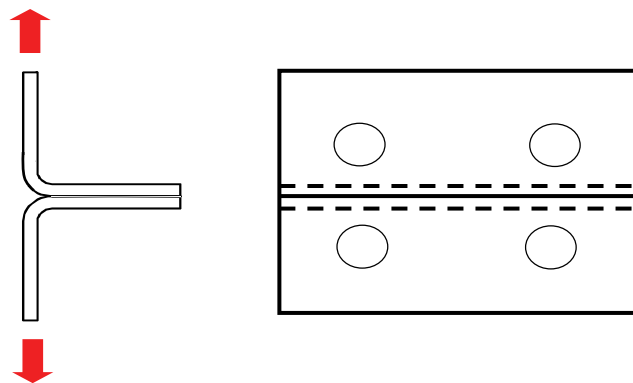*Fig. 1: Different load cases for the KSII-test*
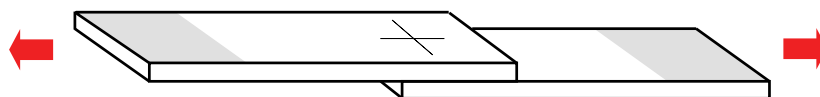
Fig. 2: Peel test specimen

Fig. 3: Lap shear specimen

2.3   Test on component level: T-section

The test cases that were shown in the last paragraph are simple specimens with one spot weld only. However, in real structures interactions by several spot welds and multi-axial stress states are dominating the behaviour. To validate the present spot weld model and to study the interaction of spot welds experiments on component level were performed. Here the so called T-section component (see

Fig. 4) is used. The structure is supported via clamping on the back side. Furthermore, it is loaded by the force F_T in transversal and F_L in longitudinal direction. The load was applied quasi-static and dynamic with a velocity of 5m/s.
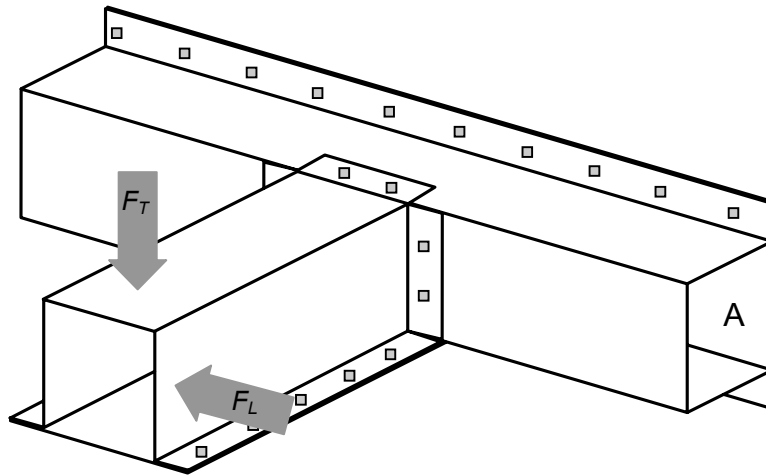

Fig. 4: T-section component

3   Numerical Investigation

The numerical model of the spot weld failure behaviour is investigated for application in full car crash simulations. The FE-models of the specimen and component experiments have to fulfil the restrictions concerning the modelling techniques of full car crash models, namely element size and type and contact formulation options used. These restrictions lead to the conclusion that the numerical model for the spotweld will consist of one element.

By fulfilling these restrictions the spot welds modelled, calibrated and validated by specimen and component tests can be directly transferred to the car model.

3.1   Base model

The simple experiments on specimen level provide the basis for further investigations on numerical modelling. Therefore the simulation models of the KSII-, peel and lap shear specimen have to cover the experiment as good as possible while still fulfilling the modelling restrictions stated above. Fig. 5 shows the finite element model of the KSII-specimen. For further investigation we will focus on the external forces F_Y^e and F_Z^e, representing the forces determined by the experiment, and on the internal forces F_Y^i and F_Z^i, representing the forces in the spot weld. Both forces will be calculated in the simulation, separately.
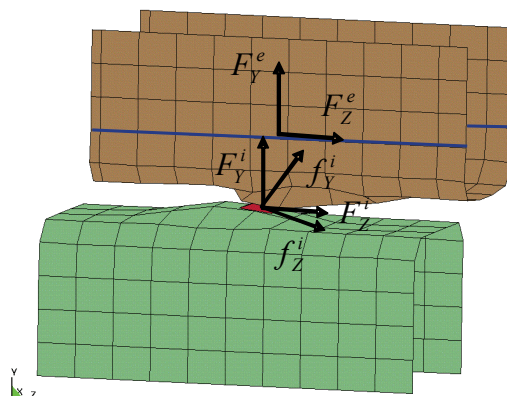

Fig. 5: External and internal forces for checking the mesh sensitivity

As described above the force-displacement characteristic of single spot welds is determined by experiments. Here the force is measured locally close to the clamping of the KSII fixation and the displacement is measured globally including the flexibility of the testing machine. Thus the force-displacement characteristic covers the overall stiffness of the testing machine and of the specimen. Therefore, the stiffness of the testing machine had to be included in the model. This could be achieved by simple beam elements on top and bottom of the specimen, where the stress-strain behaviour of the beams represents the stiffness of the testing machine.

3.2　Modelling technique

Among many different possibilities to model spot welds in crashworthiness applications, three modelling techniques have been investigated: A single beam element, a single hexahedron element and four hexahedron elements. Obviously, using a beam element is the easiest discretization effort to model spot welds with finite elements. Here we found that the overall stiffness depends strongly on the position where the beam nodes are connected to the shell surfaces. Secondly, the torsion stiffness of the beam cannot be activated, since the corresponding degree of freedom is not available in the attached shell formulation. Considering the spot weld discretization with four hexahedron elements, the small element size would decrease the time step too much and the additional mass to counterbalance this is not acceptable. The third modelling technique consists of one single hexahedron. However, the available options to model failure were found not accurate enough in most cases.

3.3　Material behaviour of MAT_100

Concerning the experiments on KSII-level we consider the 0° load case and the 90° load case to calibrate the material behaviour. In the 90° load case bending deformations of the flanges dominate the force-displacement curves, whereas the characteristic shear deformations of the spot weld dominate the behaviour of the 0° load case. Therefore the 0° load case will be taken to determine the material properties of the spot weld material model.

For modelling the material behaviour a bilinear elastic-plastic material law based on the classical vonMises-criteria is used, see Fig. 6. As input data only Young's modulus and Poisson's ratio are required for elasticity, and both yield stress and the hardening modulus for plastic range, respectively. In most cases this relatively simple material law is able to reproduce the experimental data.

The calculation of the forces/moments or stresses in the spot weld are also performed in the MAT_100 subroutine and is handled in several steps. On the basis of the strain increment the element stresses are calculated by the bilinear elastic-plastic material law. Since the MAT_SPOTWELD can only be used with reduced integration, element stresses exist only for one Gaussian point. With the element stresses the nodal forces at the bottom of the spot weld hexagon are calculated. Corrected by the hourglass forces the stress components are computed back to gain the maximum edge-stresses of an equivalent beam with circular cross section. These modified stresses not only contain shear and normal components but also a bending component. The main reason for calculation of residual stresses is the presence of a bending component which is important if we want to distinguish a symmetric normal load from a asymmetric peeling load.
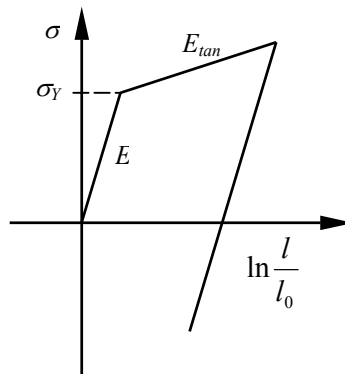
Fig. 6: Elastic-plastic material behaviour of MAT_100

Taking into account, that shear and bending ratio depend on the real thickness dimension of the spot weld, the bending and the shear stresses can be corrected by the parameter TRUE_T, which represents the true thickness.

3.4 Contact and discretization issues

First investigations were performed on detailed models to evaluate the behaviour of the spot weld discretization in different configurations (see e.g. 4]). The best case for implementing any spot weld model into a full car crash model, of course, is a configuration of non-matching flange meshes with the aim to minimize the labour intensive meshing effort.

In Fig. 7 different placements of the hexagonal element in relation to the shell elements are shown. It is shown in Fig. 8 that dependent on the solid element position and the adjusted contact thickness different contact forces between the flange shell elements develop.
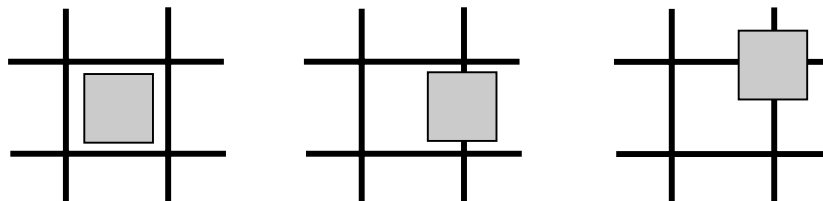

Fig. 7: Possible hexagonal vs. shell position in non-matching meshes

Fig. 8: Contact forces

In some configurations these contact forces are of artificial, parasitic nature and will disturb the internal spot weld forces (and consequently stresses etc.). Computation of the failure criterion based on these parasitic forces causes unphysical and even unpredictable failure of the solid spot weld element. In a simple test case basic investigations of the mesh sensitivity and the influence on internal forces were performed. On the basis of the numerical model of the KSII-specimen (Fig. 1) comparison of the internal and the external as well as the contact forces is possible. For the configuration of a 30° load angle and 5 m/s load velocity a mesh offset between upper and lower shell element flange in steps of 25%, 50%, 75% and 95% has been chosen. The results are documented in Fig. 9.
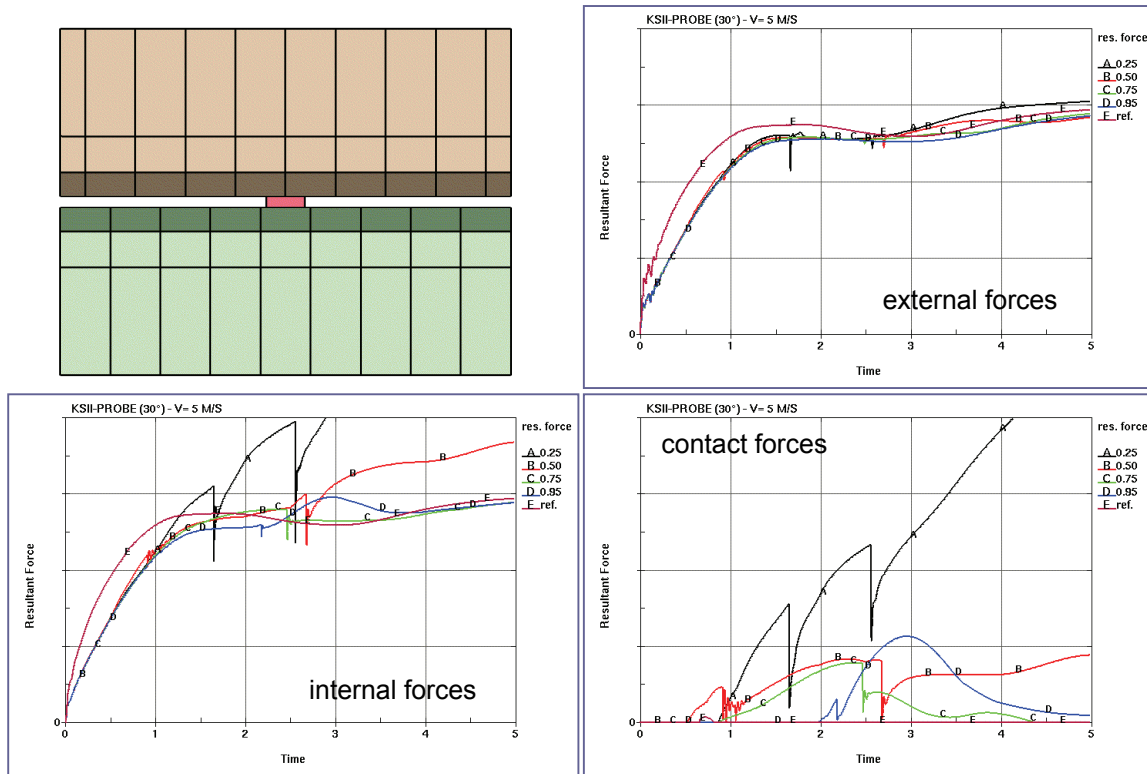
Fig. 9: Comparison of internal, external and contact forces due to mesh offset

Usually equal internal and external forces would be expected. Due to the contact forces the internal forces are disturbed and differ considerable from the external forces, especially in the case of 25% mesh offset (compare Fig. 9). Whereas the external forces are relatively robust against the mesh offset.

To prevent these parasitic contact forces from disturbing the internal spot weld forces the contact formulation was modified. If CONTACT_SPOTWELD is used, then the contact thickness of the flange shell elements can be reduced adjacent to the hexagonal element. The scaling factor is defined in CONTROL_CONTACT by the parameter SPOTHIN. With 50% reduction of the contact thickness in the vicinity of the hexagonal element (SPOTHIN = 0.5) the contact forces decrease significantly. Contact forces now occur only in cases of extreme deformation which is not relevant. The analysis of experiments show that failure of spot welds usually occur for moderate deformations.
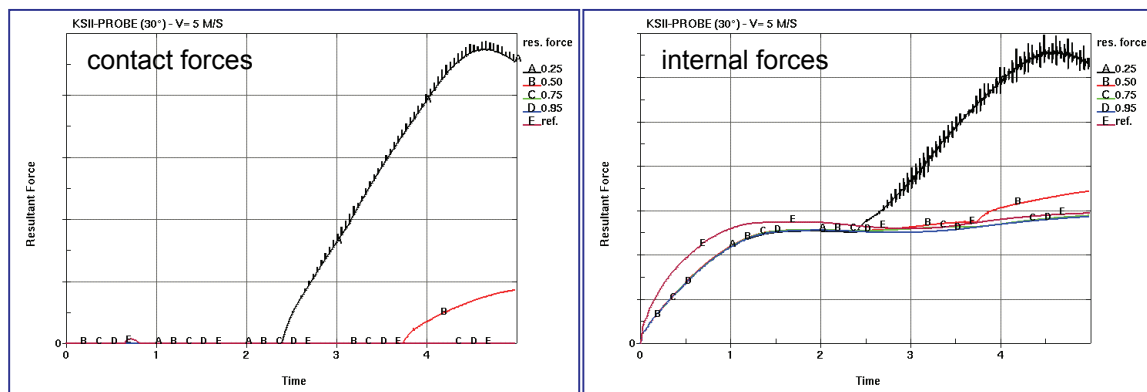

Fig. 10: Reduced contact forces

3.5   Failure behaviour

Usually stress based failure criteria are defined only in terms of normal and shear stresses. A general quadratic formulation is given by (see e.g. [5])

$$\left(\frac{\sigma}{S_N}\right)^{n_S} + \left(\frac{\tau}{S_S}\right)^{n_N} < 1 \, . \tag{1}$$

This criterion is already available in MAT_100 for hexagonal elements as well as for beam elements. In most cases the exponents n_S and n_N are chosen equal. This formulation covers the failure behaviour of the spot weld as for instance investigated in KSII-experiment setups. Concerning peel or simple shear experiments the simulations including these simple failure criteria do not match the experimental data. The spot weld fails due to bending stress in the simulation at much lower external load in comparison to the experiment. As mentioned before, the bending stress component is very important for the description of peeling dominated load cases. The herein proposed failure criterion reads therefore

$$f_{3D} = \left(\frac{\sigma_N}{S_N}\right)^{n_S} + \left(\frac{\sigma_B}{S_B}\right)^{n_B} + \left(\frac{\tau}{S_S}\right)^{n_N} < 1 \, . \tag{2}$$

The new 3D failure criterion describes a polynomial failure surface as shown in Fig. 11. The spot weld fails if the stress triple of the internal normal, bending and shear stresses is above the surface and violates Eqn. (2). Dynamic effects can be included by strain rate depended strength components. Thus Eqn. (2) is extended to

$$f_{3D} = \left(\frac{\sigma_N(\dot{\varepsilon})}{S_N(\dot{\varepsilon})}\right)^{n_S} + \left(\frac{\sigma_B(\dot{\varepsilon})}{S_B(\dot{\varepsilon})}\right)^{n_B} + \left(\frac{\tau(\dot{\varepsilon})}{S_S(\dot{\varepsilon})}\right)^{n_N} < 1 \, ,$$

where

$$S_N(\dot{\varepsilon}) = \overline{S}_N \, f_N(\dot{\varepsilon}), \ S_B(\dot{\varepsilon}) = \overline{S}_B \, f_B(\dot{\varepsilon}) \quad \text{and} \quad S_S(\dot{\varepsilon}) = \overline{S}_S \, f_S(\dot{\varepsilon}).$$

This formulation has been implemented in LS-DYNA. The strain rate functions $f_N(\dot{\varepsilon}), \ f_B(\dot{\varepsilon})$ and $f_S(\dot{\varepsilon})$ are defined by load curves.
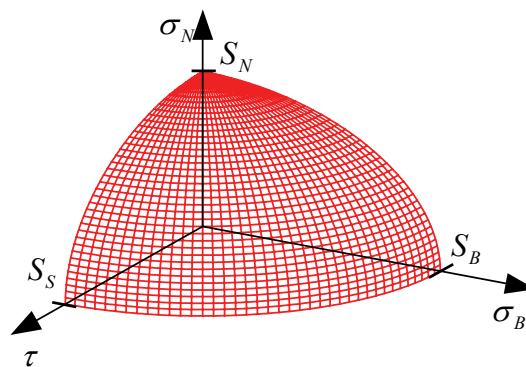

Fig. 11: 3D failure surface - according to normal, bending and shear stress

To prevent spot weld failure in case of strong oscillation effects, the failure value f_{3D} can be averaged over several cycles. In practise the spot weld diameter depends usually on the thickness of the adjacent flanges. However, at present most available pre-processing software tools create spot weld hexagons with fixed dimensions, i.e. spot weld solids with constant edge length are generated throughout the full car model. Therefore, a scaling factor has been implemented in the failure subroutine of MAT_100. Now, the user has the choice to scale the spot weld area by an individual parameter, thus allowing different spot weld dimensions without touching in-place pre-processing processes. In this context scaling the area means that the normal, shear and bending component of the failure criterion (2) will be separately corrected by the ratio of modelled and real cross section of the spot weld. Area scaling can be turned on or off by the parameter AREA_SCAL.

3.6   Consideration of damage

The forces and moments in the vicinity of the spot weld such as contact forces and internal element stresses are in equilibrium until failure of a spot weld occurs. If the spot weld element would be deleted within one single cycle, the stored elastic energy would totally be released in one step, too. In this case the load and consequently the internal stresses in adjacent spot welds would rise significantly, so that the next spot weld may fail. If this effect continues, spot weld failure can occur along the whole flange because the model does not contain energy dissipation. To prevent this mechanism and to describe the post failure behaviour more physically the following damage function is introduced:

$$\bar{\sigma} = \frac{a}{d} \sigma$$

The damage d can be calculated in two different ways, based on either plastic strain, or on the failure function f. The strain based formulation of the damage parameter d can be written as

$$d = \frac{\varepsilon - \varepsilon_p^f}{\varepsilon_p^r - \varepsilon_p^f},$$

where ε_p^f describes the plastic strain at failure time ($f=1$) and ε_p^r defines the equivalent plastic rupture strain when the element shall be eroded ($d=1$). When the normal stress dominates the stress state, spot weld failure occurs even in elastic state. In this case the yield stress is changed to the actual stress if the element fails, so that the hexagonal element begins to yield. Using the failure value f_{3D} in Eqn. (2) leads to the alternative damage formulation

$$d = \frac{f - 1}{f^r - 1}. \tag{4}$$

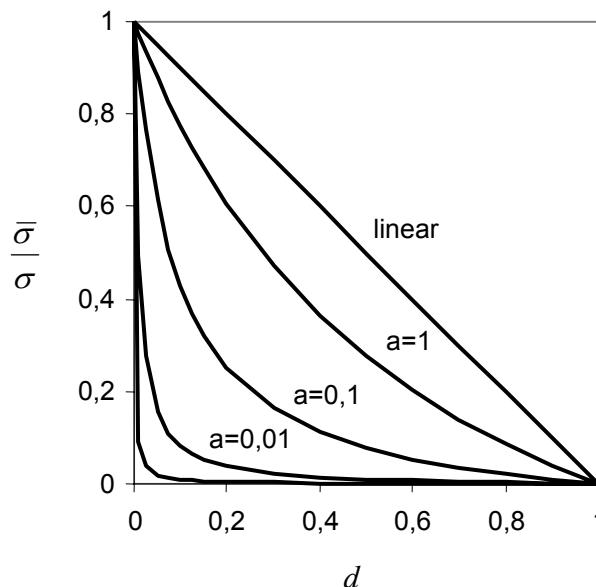In Eqn. (4) f^r represents the failure value where the element will be deleted.

Fig. 12: Damage function to describe the post failure behaviour

The shape of the damage function can be changed by the parameter *a*. The following example will show the influence and importance of the shape choice: If the flange shell elements adjacent to the spot weld solid element show plastic deformaton and, at the same time, the failure value is reached, then the stress should decrease rapidly. Otherwise if the solid element stresses are higher than those of the shell element, the stress reduction localizes in the shell elements. Thus, the solid spot weld element will not be deleted.

4   Example

First we demonstrate the new spot weld model on specimen level for a symmetric DP600 1.15mm combination of flange partners. To determine the failure parameters we used the KSII experiments at 0°, 30°, 60° and 90° as well as the peeling test. All these experiments were considered in a calibration procedure based on the least square method. The calibration process has been performed using LS-OPT. In Fig. 13 the calculated failure surface with the stress triples of the KSII and peel experiments are shown.
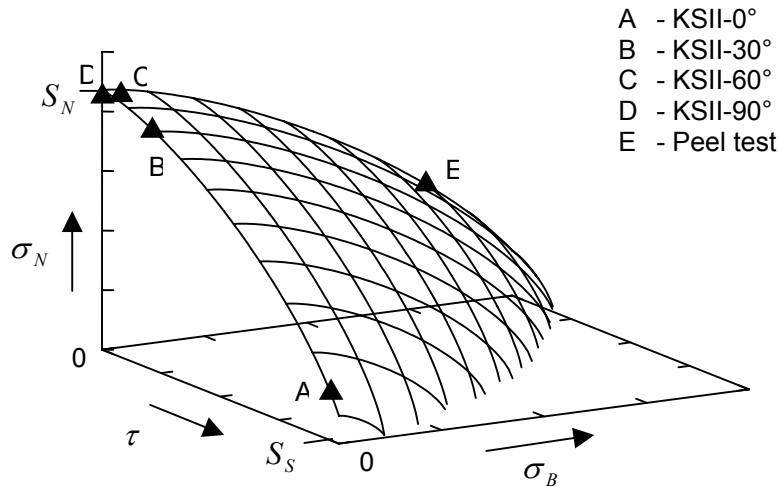

A - KSII-0°
B - KSII-30°
C - KSII-60°
D - KSII-90°
E - Peel test

Fig. 13: Failure surface with stress triples

It can be seen that the KSII experiments are used to gain the exponents for the optimal shape of the failure criterion. In these cases the components of bending stress are nearly negligible for KSII specimen. The peeling test is needed to derive the bending strength of the spot weld model. Hence the calculation of the failure criterion parameters based on the experiments as shown in Fig. 13 delivers appropriate correlation of experimental data and simulation.
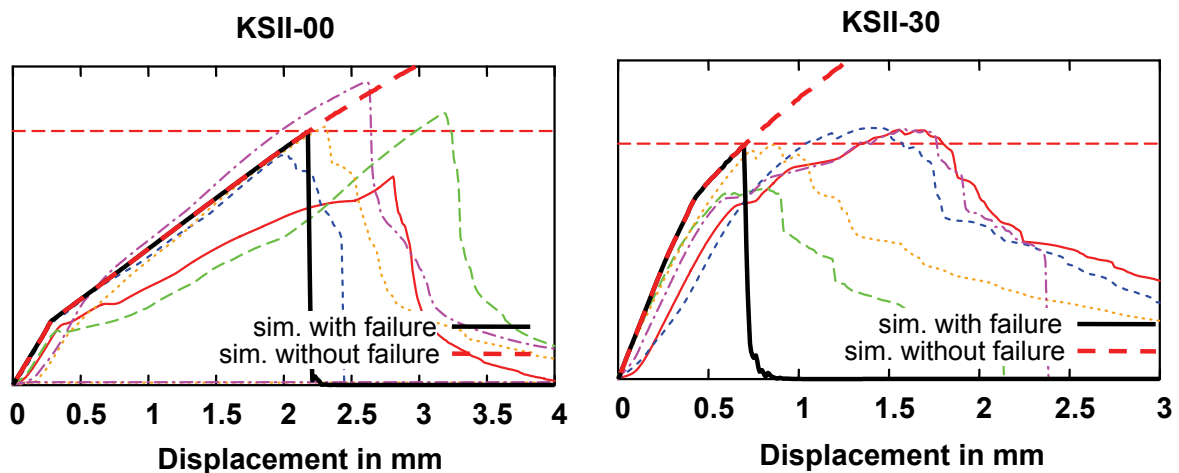

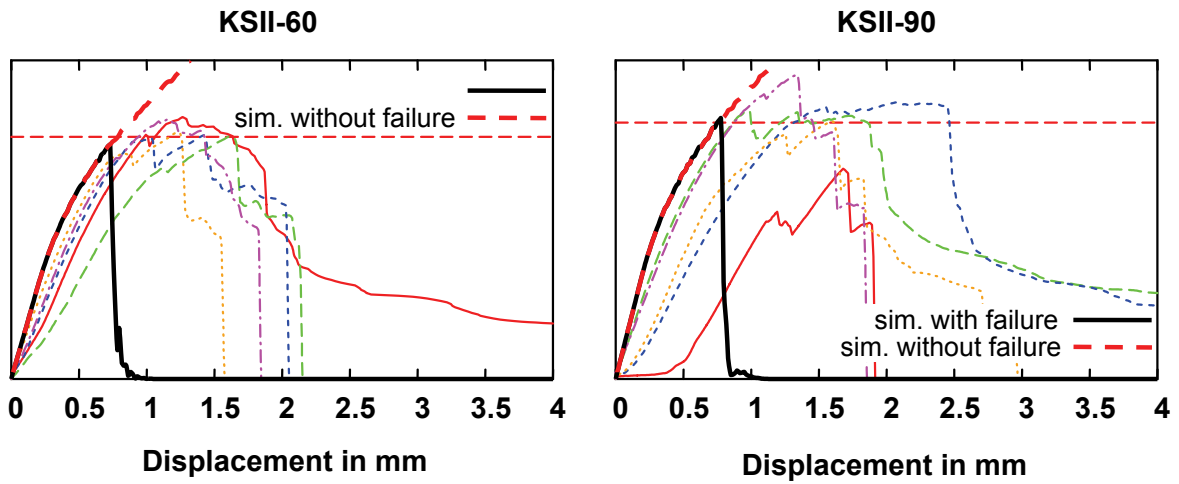*Fig. 14 Comparison of experiment and simulation for ksii-0° and ksii-30°*

KSII-60

KSII-90

Fig. 15 Comparison of experiment and simulation for ksii-60° and ksii-90°
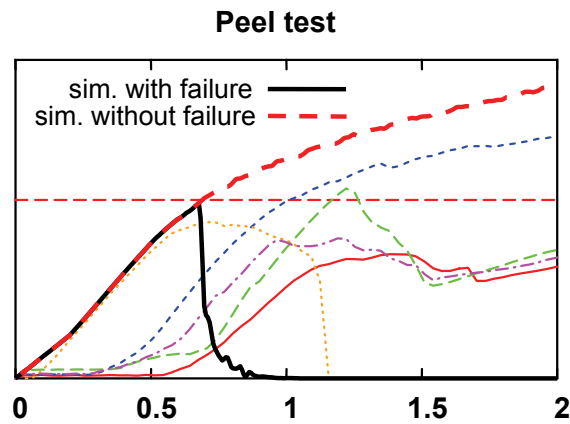
Peel test

Fig. 16 Comparison of experiment and simulation for peeling

The failure criterion with the material specific failure values are validated on the T-component with lateral load configuration. The forces will be measured with two load cells at the clamping and the displacement is measured directly at the ram.
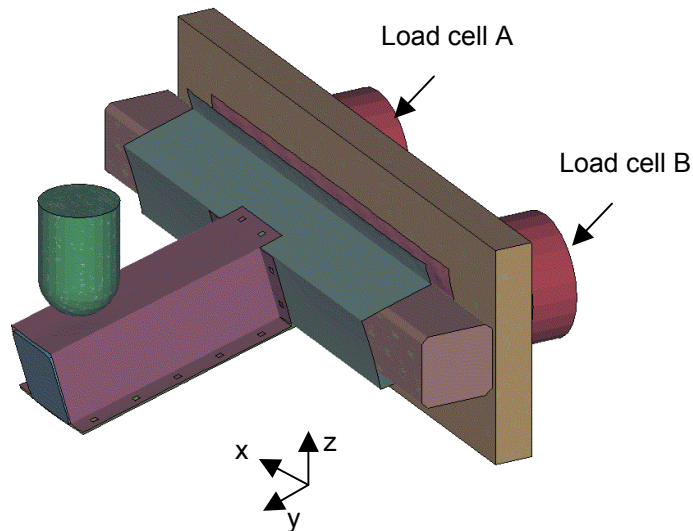

Fig. 17: T-Component after spot weld failure
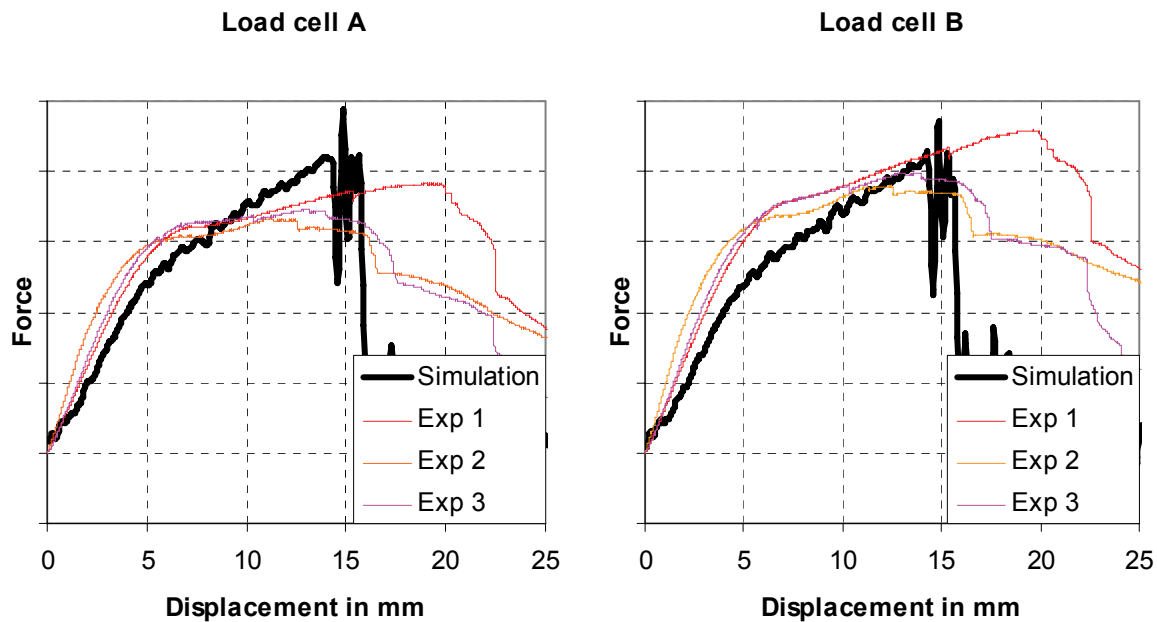
Load cell A   Load cell B

Fig. 18: Force-displacement-characteristics of T-component

The force characteristics in z-direction of the T-component (see Fig. 17) in the simulation and the experiments are compared in Fig. 18 and show good correlation. The spot weld failure on the upper flange occurs at the same critical load and displacement. Since the spot welds are mainly loaded by normal forces in the upper flange, the material behaviour of the spot weld is elastic at failure time. Therefore the force characteristic of the simulation is stiffer before failure and declines faster after failure in comparison to the experiments. Especially the damage functions ensure realistic post failure behaviour in the simulation.

5   Conclusion

In this paper we presented a useful modelling technique to describe the behaviour of spot weld in car crash simulations. The investigations on the contact formulations were necessary for the correct evaluation of spot weld forces and stresses. On the basis of the spot weld stresses we derived a new failure criterion to model the spot weld failure behaviour in car crash simulations. It could be shown that it is essential to enhance the existing failure criterion by bending terms to cover all load types.
A realistic description of the spot weld behaviour in complex component and car crash simulations is obtained by introducing the new failure criterion in combination with the modified contact formulation.

6   Literature

[1]   Hahn O., K. Özdem, M. Oeter: Abschlußbericht: „Experimentelle Bestimmung und rechnerische Vorhersage des Tragverhaltens punktgeschweißter Bauteile aus Stahlblechverbindungen unter Crashbelastung mit Hilfe von Ingenieurkonzepten", FAT/ AVIF A172; Februar 2004

[2]   Hahn, O., J. R. Kurzok, A. Rhode: Untersuchungen zur Übertragung von Kennwerten einer punktgeschweißten Einelementprobe auf Mehrpunktprüfkörper und Bauteile, FAT-Schriftenreihe Nr. 146, 1999

[3]   Rupp, A. et al.: Ermittelung ertragbarer Beanspruchung am Schweißpunkt auf der Basis übertragbarer Schnittgrößen. FAT Schriftenreihe 111, 1994

[4]   Sommer S., Sun D-Z., Modelling of the failure behaviour of spot welds under crash loading, International Symposium Crashworthiness of Light-Weight Automotive Structures, Trondheim, 2004.

[5]   Zhang, S.: Approximate Stress Formulas for Multiaxial Spot Weld Specimen, American Spot Weld Society, July 2001

[6]   N.N.: LS-DYNA Nonlinear Dynamic Analysis of Structures, User's Manual, Livermore Software Technology Cooperation, Livermore, California, 2005